The influence of image set size on the resulting super-resolution image

Yegor Goshin
Samara National Research University
Samara, Russia
goshine@yandex.ru

Daria Arkhipova
Samara National Research University
Samara, Russia
mazyaikinadasha@gmail.com

Anton Kotov
Samara National Research University; Image Processing Systems Institute of RAS - Branch of the FSRC "Crystallography and Photonics" RAS
Samara, Russia
kotov@ssau.ru

Daria Aksenova
Samara National Research University
Samara, Russia
darinaksena@gmail.com

***Abstract*—In this paper, we consider super-resolution image reconstruction using the method of projections onto convex sets. We explore an influence of input image set size on the result of super-resolution reconstruction. We propose an indicator value as a ratio between the number of images in the set and the square of upscale factor of reconstruction. The method of convex projections was implemented using the Python programming language. The experiments were conducted on the Standard test images from TESTIMAGES project set. The results and future plan for improving the POCS method for super-resolution reconstruction are discussed in the final part of the paper.**

Keywords—super-resolution, the method of projections onto convex sets

I. Introduction

Super-resolution (SR) of an image provides a high pixel density and, therefore, more details about the object can be captured. The super-resolution problem is raised in computer vision in regard to pattern recognition and image analysis [1] [2], in the task of medical imaging [3] and the Earth remote sensing [4]. CNN-based super-resolution algorithms were successfully applied to image super-resolution problem [5], [6]. These algorithms learn representations from large training databases of high- and low-resolution image pairs or exploit self-similarities within an image [7]. Super-resolution imaging devices are expensive, and their usage is not always possible due to sensor limitations and optical technology (e.g., thermal imaging systems [8]). Image processing algorithms partially solve these problems by simplifying the system for obtaining images due to the greater computational load. Existing methods for improving image resolution fall into two large categories: linear [9] and adaptive [10].

Linear methods, such as bicubic interpolation [11], are easy to implement but do not allow us to completely extract information from source images. The use of adaptive methods provides a better result. Among the technologies for improving image resolution from the set of images, super-resolution technology is the most effective.

Conventional approaches to generating super-resolution images require multiple low-resolution images of the same scene, which are aligned with sub-pixel accuracy [12]. In this paper, we study a method for constructing super-resolution image using projections onto convex sets (POCS) [13].

II. Problem Statement

The problem of the super-resolution reconstruction can be formulated as follows. There is a set of N low-resolution images of the same scene. Each low-resolution image is obtained by downsampling of the high-resolution image (Fig. 1). In matrix form this observation model image is written as follows:

$$\begin{bmatrix} \boldsymbol{b_1} \\ \vdots \\ \boldsymbol{b_N} \end{bmatrix} = \begin{bmatrix} \boldsymbol{D_1} \cdot \boldsymbol{B_1} \cdot \boldsymbol{W_1} \\ \vdots \\ \boldsymbol{D_N} \cdot \boldsymbol{B_N} \cdot \boldsymbol{W_N} \end{bmatrix} \boldsymbol{X} + \begin{bmatrix} \boldsymbol{e_1} \\ \vdots \\ \boldsymbol{e_N} \end{bmatrix} = \begin{bmatrix} \boldsymbol{A_1} \\ \vdots \\ \boldsymbol{A_N} \end{bmatrix} \boldsymbol{X} + \begin{bmatrix} \boldsymbol{e_1} \\ \vdots \\ \boldsymbol{e_N} \end{bmatrix} \tag{1}$$

where $\boldsymbol{b_i}$ $(i = \overline{1,n})$ are the low-resolution images with the size of $M \times M$ pixels, $\boldsymbol{D}$ is a subsampling matrix with the size of $M^2 \times P^2$ pixels; $\boldsymbol{B}$ is a blurring matrix with the size of $P^2 \times P^2$ (the matrix is evaluated from the point spread function (PSF) [14]); $\boldsymbol{W}$ is a geometric transfer matrix with the size of $P^2 \times P^2$ pixels [15]; $\boldsymbol{X}$ is a high-resolution image $P \times P$; $\boldsymbol{e}$ is a Gaussian noise.

a)

b)

Fig. 1. a) Test image; b) Rotated, blured and downsampled low-resolution images.

In this paper, we resample super-resolution image using the POCS method. The operator of the corresponding convex set of constraints projects points from the solution space onto the nearest point on the surface of this convex set. After a finite number of iterations, a solution to the set of intersections comes to a convex set of constraints.

The algorithm can be represented in the form of the following steps.

1. Evaluation of the interpolated low-resolution image.

2. Calculation of the displacement (motion compensation) of pixels on each low-resolution. The correspondence between high and low resolution images is given as

$$g(m_1, m_2, l) = \sum_{n_1,n_2} f(n_1, n_2) h(n_1, n_2; m_1', m_2' l) + n(m_1, m_2 l),$$

where (m_1, m_2) is a point of the interpolated low-resolution image, and (n_1, n_2) is a corresponding point into high-resolution image.

3. Obtaining a pixel position on low- and high-resolution images.

Then we evaluate the $h(n_1, n_2; m_1', m_2' l)$ parameter which is a value of point spread function according to the pixel position. The obtained low-resolution image $g(m_1, m_2, l)$ can be constrained by a convex set $\mathrm{C}_{n_1,n_2,k}$. Therefore:

$$\mathrm{C}_{n_1,n_2,k} = \{f(m_1, m_2, l): |r^{(f)}(n_1, n_2, k) \leq \partial_0(n_1, n_2, k)|\}$$
$$0 \leq n_1, n_2 \leq N-1, k = 1, \dots, L$$

Projection $P(n_1, n_2, k)x[m_1, m_2, l]$ onto $C(n_1, n_2, k)$ in arbitrary point $x(m_1, m_2, l)$ can be represented as:

$$P(n_1, n_2, k)x[m_1, m_2, l] =$$
$$\begin{cases} x(m_1, m_2, l) + \frac{r^{(x)}(n_1,n_2,k) - \partial_0(n_1,n_2,k)}{\sum\sum h^2(n_1,n_2;m_1',m_2' l)} h(n_1, n_2; m_1\ , m_2\ l) \\ r^{(x)}(n_1, n_2, k) > \partial_0(n_1, n_2, k) \\ x(m_1, m_2, l) \\ -\partial_0(n_1, n_2, k) < r^{(x)}(n_1, n_2, k) < \partial_0(n_1, n_2, k) \\ x(m_1, m_2, l) + \frac{r^{(x)}(n_1,n_2,k) + \partial_0(n_1,n_2,k)}{\sum\sum h^2(n_1,n_2;m_1',m_2' l)} h(n_1, n_2; m_1\ , m_2\ l) \\ r^{(x)}(n_1, n_2, k) < -\partial_0(n_1, n_2, k) \end{cases}$$

We estimate a residual between the test image and the reconstructed using the described algorithm. The residual formula can be written as:

$$r^{(f)}(n_1, n_2, k) = g(n_1, n_2, l) - \sum f(m_1, m_2, l) \cdot h(n_1, n_2; m_1', m_2' l)$$

where $h(n_1, n_2; m_1', m_2' l)$ is an impulse response coefficient, ∂_0 is a confidence level for the observed results. These parameters define high-resolution images that correspond to low-resolution images within a confidence interval.

4. Iterative repetition of the second step until the stop condition is met.

With the use of a projection operator, the estimated value $f(m_1, m_2, l)$ of the high-resolution image can be found using all low-resolution images by performing some iterations:

$$\hat{f}^{(i+1)}(m_1, m_2, l) = T_\lambda \tilde{T}[\hat{f}^{(i)}(m_1, m_2, l)] \;\; i = 0,1, \dots,$$

where $\tilde{T}$ is a combination of all projection operators associated with $C(n_1, n_2, k)$. The initial approximation $f^0(m_1, m_2, l)$ is obtained by bilinear interpolation.

We conducted a research about super-resolution image reconstruction using the method of POCS. An influence the parameters of image set formation and parameters of an above algorithm to the super-resolution reconstruction was investigated.

III. Experimental Results and Analisys

In this paper, an experimental study of the influence of the number of input images on the result of image reconstruction was carried out for different image scaling parameters.

Images from the TESTIMAGES project set [16], [17] were used as test images. Rotation, translation, blurring and downsampling were performed to generate low-resolution raw images for the experiment. The size of the blurring window was the same as the downsampling scale. The SURF algorithm was used to align the images. The method of convex projections was implemented using Python programming language with libraries OpenCV [18] and NumPy[19].

The value of the relative "information completeness" has been proposed as a universal measure of the number of images in a set. This indicator was calculated as

$$p = \frac{\{number\ of\ images\ in\ the\ set\}}{\{image\ scale\ factor\}^2} = \frac{N}{S^2}$$

This value allows us to assess the degree of "completeness" of information. Evidently, in a randomly generated set, an indicator value equal to 1 does not guarantee sufficient information to restore an absolutely accurate original image. However, it will be further shown that this indicator is quite meaningful.

Also, to assess the effect of the matching stage on the result, a test reconstruction was carried out using the same algorithm (POCS), but under the assumption that the image matching parameters are known (these parameters were stored at the low-resolution image generation stage). Fig. 2 shows dependence of the peak signal-to-noise ratio (PSNR) and the structural similarity index (SSIM values on propose for different scale values for both experiments.

In Fig. 3, we demonstrate the results of described algorithm for the scale factor rate equal to 0.85.

The reconstructed image shows that the quality of super-resolution image is better than the quality of the low-resolution image.

IV. Discussion

The experiment showed that in a perfect scenario (when the matching parameters are known) it is best to set the resolution upscaling parameter *S* so that the size of the set of images *N* satisfies the following constraints:

$$0.4 \leq \frac{N}{S^2}.$$

Second experiment showed that in a realistic scenario (for unknown estimated matching parameters), values of PSNR and SSIM are less than in the perfect scenario. Moreover, adding images above the $p = 0.85$ impair the result further. This is due to the fact that the matching itself does not always provide quite accurate result and POCS algorithm is not robust and requires additional procedures to filter erroneously matched images. So we add another restriction:

$$0.35 \leq \frac{N}{S^2} \leq 0.85,$$

or, equivalently,

$$1.08\sqrt{N} \leq S \leq 1.69\sqrt{N}.$$

We plan to investigate POCS robustness later in our further research.

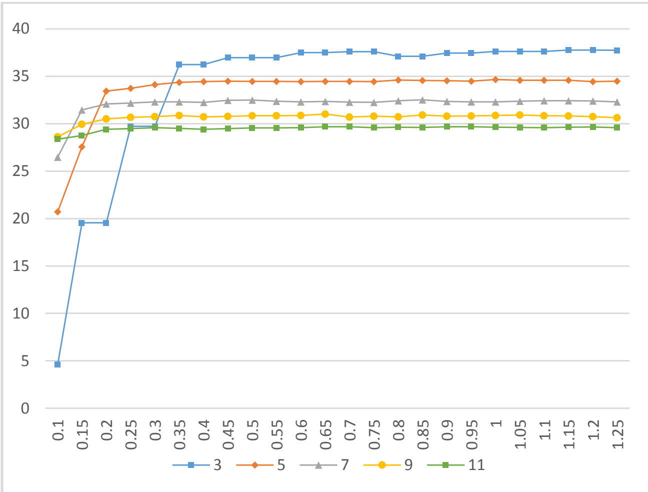

a) PSNR values for known matching parameters

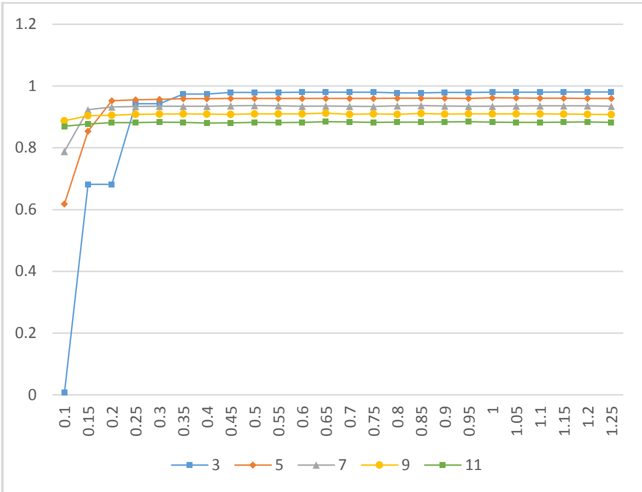

b) SSIM values for known matching parameters

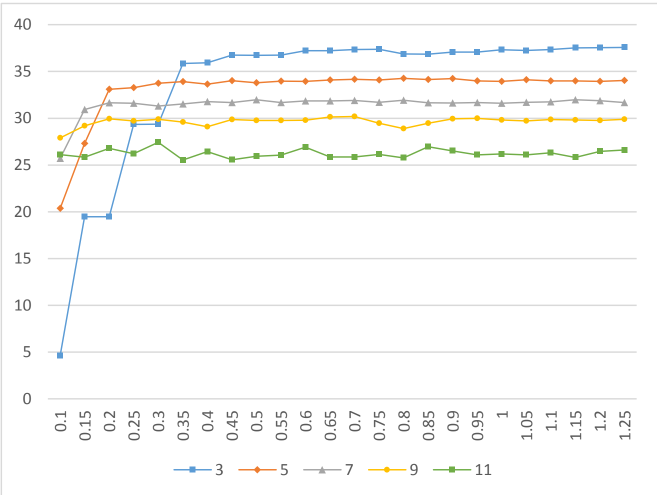

c) PSNR values for estimated matching parameters

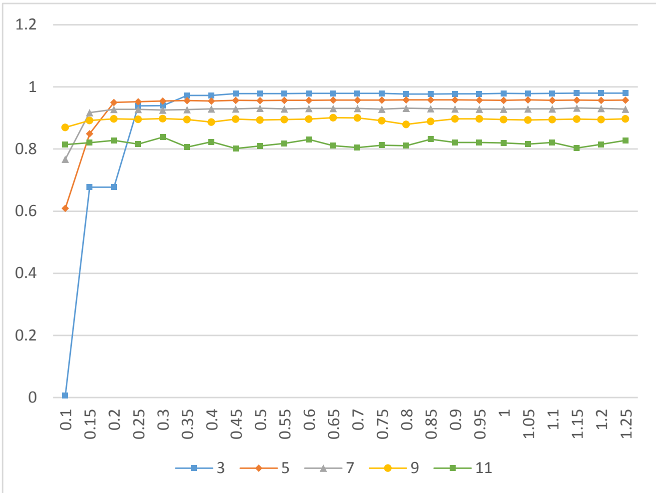

d) SSIM values for estimated matching parameters

Fig. 2. PSNR and SSIM values for different scale values for both experiments.

Fig. 3. Results of described algorithm. From left to right: Test image (original data), Low-resolution image (synthetically degrading the original data), Reconstructed image (p=0.85).

V. Conclusion

In this work, we have discussed the influence of the parameters of image set formation and the parameters of an algorithm on reconstruction. We have developed the recommendations for the super-resolution reconstruction problem using the method of POCS.

Acknowledgment

The research was carried out within the state assignment theme #0777-2020-0017, was partly financially supported by the RFBR under grant #17-29-03112 and #18-07-01390, and by the Ministry of Science and Higher Education.

References

[1] V.V Myasnikov, “Reconstruction of functions and digital images using sign representations,” Computer Optics, vol. 43, no. 6, pp. 1041-1052, 2019. DOI: 10.18287/2412-6179-2019-43-6-1041-1052.

[2] H. Takeda, P. Milanfar, M. Protter and M. Elad, “Super-resolution without explicit subpixel motion estimation,” IEEE Transactions on Image Processing, vol. 18, pp. 1958-1975, 2009.

[3] D.V. Kirsh, A.S. Shirokanev and A.V. Kupriyanov, “Algorithm of reconstruction of a three-dimensional crystal structure from two-dimensional projections,” Computer Optics, vol. 43, no. 2, pp. 324-331, 2019. DOI: 10.18287/2412-6179-2019-43-2-324-331.

[4] L. Luo and J. Xiao, “Super-resolution enhancement of UAV images based on fractional calculus and POCS,” Geo-spatial Information Science, pp. 56-66, 2018.

[5] C. Lanaras, J. Bioucas-Dias, S. Galliani, E.Baltsavias and K. Schindler, “Super-resolution of Sentinel-2 images: Learning a globally applicable deep neural network,” ISPRS Journal of Photogrammetry and Remote Sensing, vol. 146, pp. 305-319, 2018.

[6] A. Kappeler, S. Yoo, Q. Dai and A. K. Katsaggelos, "Video super-resolution with convolutional neural networks," IEEE Transactions on Computational Imaging, vol. 2, no. 2, pp. 109-122, 2016.

[7] S. Schulter, C. Leistner and H. Bischof, “Fast and accurate image upscaling with super-resolution forests,” Proc. IEEE Conf. Comput. Vis. Pattern Recog., pp. 3791-3799, 2015.

[8] J.A. Ratches, "Static Performance Model for Thermal Imaging Systems," Optical Engineering, vol. 15, no. 6, 1976.

[9] R. Roesser, "A discrete state-space model for linear image processing," IEEE Transactions on Automatic Control, vol. 20, no. 1, pp. 359-362, 1975.

[10] J.W. Hwang and H.S. Lee, "Adaptive image interpolation based on local gradient features," IEEE Signal Processing Letters, vol. 11, no. 3, pp. 359-362, 2004.

[11] M.A. Nuno-Maganda and M.O. Arias-Estrada, "Real-time FPGA-based architecture for bicubic interpolation: an application for digital image scaling," International Conference on Reconfigurable Computing and FPGAs (ReConFig'05), Puebla City, pp. 8, 2005.

[12] J. Yang, J. Wright, T.S. Huang and Y. Ma, “Image super-resolution via sparse representation,” IEEE transactions on image processing, vol. 19, no. 11, pp. 2861-2873, 2010.

[13] F.W. Wheeler, R.T. Hoctor and E.B. Barrett, “Super-resolution image synthesis using projections onto convex sets in the frequency domain,” Computational Imaging III, International Society for Optics and Photonics, vol. 5674, pp. 479-490, 2005.

[14] F.N. Mboula, J.L. Starck, S. Ronayette, K. Okumura and J. Amiaux, “Super-resolution method using sparse regularization for point-spread function recovery,” Astronomy & Astrophysics, vol. 575, p. A86, 2015.

[15] M. Sattarivand, M. Kusano, I. Poon and C. Caldwell, “Symmetric geometric transfer matrix partial volume correction for PET imaging: principle, validation and robustness,” Physics in Medicine & Biology, vol. 57, no. 21, 7101, 2012.

[16] N. Asuni and A. Giachetti, "TESTIMAGES: A Large Data Archive For Display and Algorithm Testing," Journal of Graphics Tools, vol. 17, no. 4, pp. 113-125, 2015.

[17] N. Asuni and A. Giachetti, "TESTIMAGES: a large-scale archive for testing visual devices and basic image processing algorithms," STAG - Smart Tools & Apps for Graphics Conference, 2014.

[18] G. Bradski and A. Kaehler, “Learning OpenCV: Computer vision with the OpenCV library,” O'Reilly Media, Inc.,” 2008.

[19] S. van der Walt, S. C. Colbert and G. Varoquaux, "The NumPy Array: A Structure for Efficient Numerical Computation," Computing in Science & Engineering, vol. 13, no. 2, pp. 22-30, 2011. DOI: 10.1109/MCSE.2011.37.

.